

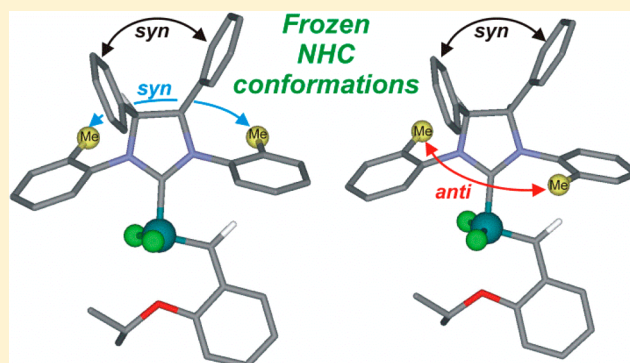
Ruthenium Olefin Metathesis Catalysts with Frozen NHC Ligand Conformations

Alessandra Perfetto, Chiara Costabile, Pasquale Longo, and Fabia Grisi*

Dipartimento di Chimica e Biologia, Università di Salerno, Via Giovanni Paolo II 132, I-84084 Fisciano, Salerno, Italy

S Supporting Information

ABSTRACT: The catalytic behavior of Grubbs and Hoveyda–Grubbs II type ruthenium complexes bearing N-heterocyclic carbene (NHC) ligands with *syn*-phenyl groups on the backbone and *syn*- or *anti*-oriented *o*-tolyl N-substituents was evaluated in a series of olefin metathesis transformations. Further advance in the synthesis of the best-performing *syn* catalysts and a deeper investigation into the solution-state structure of the Hoveyda–Grubbs type II complex with *anti* *N*-tolyl groups by 2D-NMR and DFT studies are also reported. Of particular interest, *syn* complexes emerged among the best-performing catalysts in all of the explored metathesis reactions, especially in the ring-closing metathesis (RCM) of hindered olefins, allowing also for the difficult formation of macrocyclic trisubstituted alkenes. An important unexpected result was obtained in the RCM of linalool, where both *syn* and *anti* catalysts appeared to be involved in the dehydration reaction of the cyclization product (1-methylcyclopent-2-en-1-ol). This process allowed for the formation of well-defined mixtures of methylcyclopentadiene isomers, which represent valuable precursors for the synthesis of renewable high-density fuels.



INTRODUCTION

Catalytic olefin metathesis has become one of the most powerful carbon–carbon bond-forming reactions currently available to the synthetic chemist.¹ In particular, the development of well-defined ruthenium alkylidene complexes (e.g., 1–4, Chart 1) has broadened the scope and utility of the olefin metathesis reaction in the synthesis of small molecules, preparation of natural products, and construction of polymers.^{2,3}

To allow an even more extensive use of metathesis chemistry, the design of effective catalysts that are readily available, easy to handle, reliable, and highly selective continues to be crucial. Indeed, still diverse metathesis applications such as asymmetric,⁴ sterically demanding,⁵ or aqueous⁶ transformations can be improved by identifying more suitable catalysts. Recent progress in ruthenium olefin metathesis catalysts is undoubtedly related to the modification of the N-heterocyclic carbene (NHC) ligand architecture of the classical Grubbs II and Hoveyda–Grubbs II complexes, which has produced a vast amount of structural motifs of NHCs directly influencing the catalyst's performance. For example, the fine tuning of the electronic and steric properties of the substituents on the nitrogen atoms and/or the backbone of NHCs has had a significant impact on catalyst activity, stability, and selectivity in several metathesis applications.^{4b,f,7}

Recent work in our laboratories has led to the identification of a class of ruthenium catalysts bearing NHCs with different backbone configuration (see 5–8, Chart 2).⁸ The complexes incorporating *syn*-related methyl groups on the NHC backbone

(5 and 6) have been found to better perform ring-closing metathesis (RCM) reactions of olefins in comparison to their *anti* analogues (7 and 8) and, more significantly, the *syn* complexes 5a and 6a with reduced bulk on the nitrogen atoms (*o*-tolyl N-substituents) can be counted among the most efficient catalysts in the RCM of sterically demanding substrates.⁸

The role of the NHC backbone configuration has been investigated through experimental and theoretical studies, and the origin of the enhanced reactivity observed for *syn* catalysts has been attributed to a preferential *syn* orientation of the *N*-tolyl rings imposed by the *syn* disposal of methyl groups on the backbone. This conformation of the NHC ligand provides a more sterically accessible face of the catalyst that facilitates the approach of hindered substrates.^{8,9} In a preliminary communication,¹⁰ we reported on the synthesis of novel ruthenium catalysts featuring an NHC ligand with *syn* phenyl groups on the backbone and *o*-tolyl N-substituents (9 and 10, Chart 3). The increased steric pressure of the NHC-backbone phenyl substituents on the *N*-tolyl rings allowed for the separation of ruthenium complexes with different *N*-tolyl conformations and different reactivity in RCM reactions.

The superior performance of the isomers with *syn*-oriented *N*-tolyl groups (*syn*-9 and *syn*-10) furnished incontrovertible evidence for the importance of correctly oriented *N*-aryl groups

Received: February 7, 2014

Chart 1. Well-Defined Ruthenium Benzylidene Catalysts

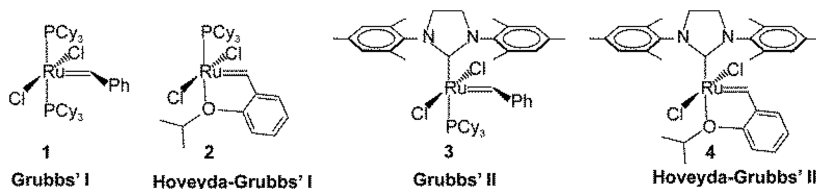
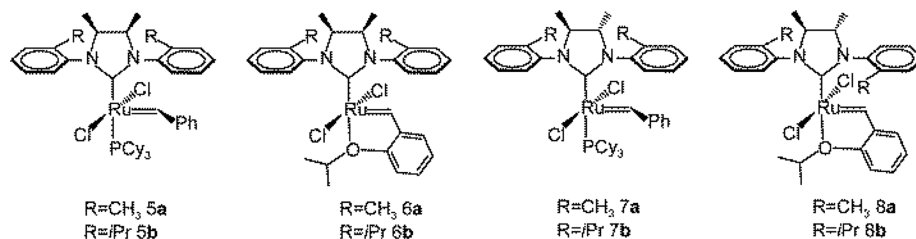
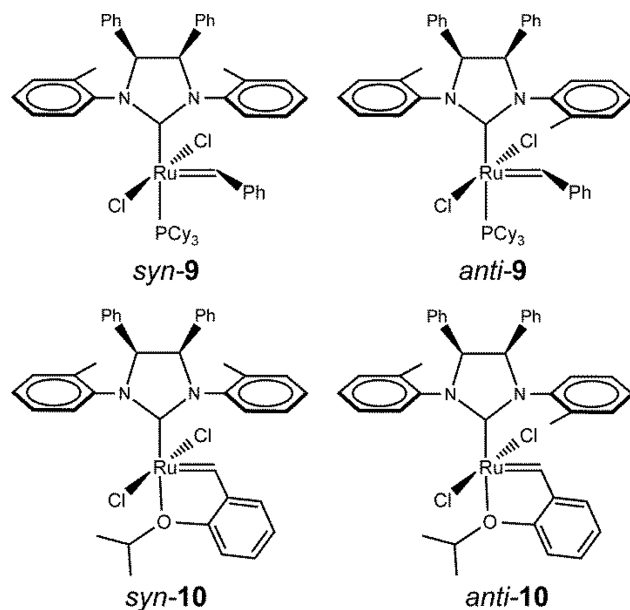
Chart 2. NHC Backbone and *N*-Aryl-Substituted Ruthenium Complexes

Chart 3. Ruthenium Catalysts with Frozen NHC Conformations



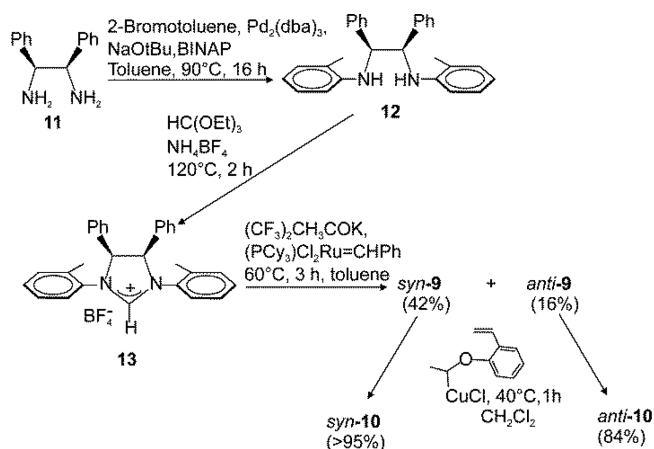
to successfully accomplish RCM reactions, leading to unprecedented results in the formation of tetrasubstituted alkenes.

To obtain a more complete picture on the catalytic behavior of Ru complexes **9** and **10** with frozen NHC conformations, we give herein a full overview on RCM studies as well as on other metathesis transformations such as ring-opening metathesis polymerization (ROMP) and cross-metathesis (CM). In addition, we describe a facile and convenient access to the highly stable and extremely active *syn*-**9** and *syn*-**10** isomers through well-known synthetic protocols, thus rendering these catalysts actually attractive for application in catalysis.

RESULTS AND DISCUSSION

Synthesis and Characterization of Catalysts **9** and **10**.

As reported in our previous work,¹⁰ the synthesis of the phosphine-containing complex **9** was easily accomplished in three steps by following the synthetic procedure^{4d} reported in Scheme 1. Chromatographic workup allowed for the isolation of two distinct isomers, which were identified as *syn*-**9** and *anti*-**9** by

Scheme 1. Synthesis of Complexes **9** and **10**

NMR analysis. Both these precatalysts are stable in a solid form as well as in solution, where the retention of the benzylidene signal, monitored by ¹H NMR spectroscopy, is observed over the course of 1 week for *syn*-**9** and 3 days for *anti*-**9**.

Starting from these phosphine-based complexes, Ru precatalysts *syn*-**10** and *anti*-**10**, bearing a chelating benzylidene ether ligand, were readily obtained from the reaction with isopropoxystyrene in the presence of CuCl as phosphine scavenger (Scheme 1).¹¹ Complexes *syn*-**10** and *anti*-**10** are highly air and moisture stable both in the solid state and in solution for extended periods of time.¹²

Solution-state structures of complex **10** were determined by NMR analyses. Only one isomer for *syn*-**10** was observed in solution, which was unambiguously identified by X-ray structure analysis.¹⁰ ¹H and ¹³C NMR analysis of *anti*-**10** revealed the presence of two isomers, corresponding to the opposite arrangement of the *anti*-oriented *N*-tolyl groups of the NHC ring.

According to density functional theory (DFT) studies on the complex stability, four minimum-energy structures were located for complex **10**. In Figure 1, the internal and free energies in benzene are reported.

The lowest energy structure **10A** corresponds to the most abundant isomer, *syn*-**10**, characterized by X-ray diffraction as well. Structure **10D** is not experimentally observed very likely

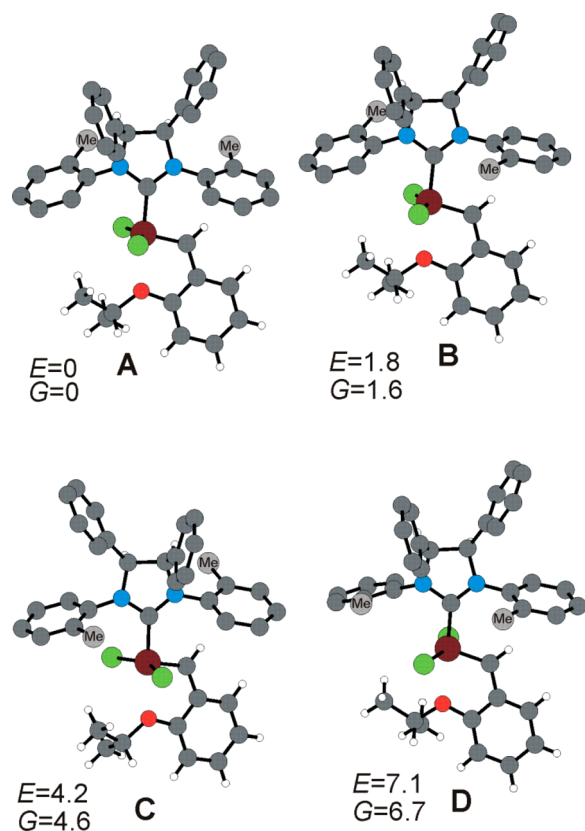


Figure 1. Isomers of complex **10**. For each structure internal and free energies in benzene, obtained by DFT calculations, are reported in kcal mol⁻¹.

because of its high energy. As for the remaining two isomers, **10B** was found to be more stable than **10C**.¹⁰

2D-NOESY/EXSY experiments displayed chemical exchange at room temperature between the major (**10B**) and minor (**10C**) forms of *anti*-**10**. Exchange cross peaks observed in the EXSY spectrum of *anti*-**10** allowed us to evaluate as 1.35 s⁻¹ the rate constant for the **10B** → **10C** direct travel, corresponding to a free energy of activation of 17.3 kcal mol⁻¹, while a rate constant of 3.85 s⁻¹ was evaluated for the **10C** → **10B** inverse run ($\Delta G^\ddagger = 16.6$ kcal mol⁻¹) (see the Supporting Information).

Exchange between **10B** and **10C** can, in principle, occur through rotation of the NHC ligand. More in detail, 180° NHC rotation around the C–Ru bond would lead to isomer **10B**, as depicted in Figure 1, to the enantiomer of isomer **C**, as depicted in the same figure. To support this hypothesis, experimental exchange barriers were compared with theoretical NHC rotational barriers calculated by DFT. Starting from the most stable isomer, **10B**, clockwise as well as counterclockwise NHC rotational barriers were located, and transition state (TS) structures have been reported in Figure 2. Internal and free TS energies in the gas phase and benzene related to isomer **10B** are shown in Table 1.

According to our studies, the lowest NHC rotational barrier corresponds to a counterclockwise (**10BC**^{-‡}) rotation of the NHC around the C–Ru bond, which passes through a TS with the backbone phenyl groups on the same side of the alkylidene ligand. The calculated free energy barrier in benzene is 16.4 kcal/mol. A clockwise rotational barrier requires about 1.6 kcal/mol more, due to the steric interaction of one of the methyl groups of the *N*-aryl group that get stuck at short distances (3.3–3.4 Å)

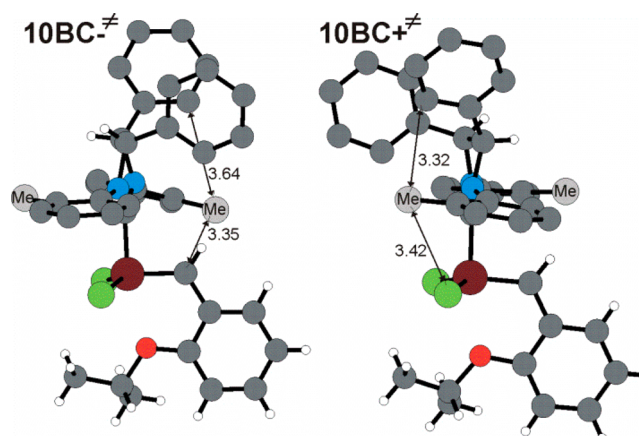


Figure 2. TS NHC rotational counterclockwise (left, **10BC**^{-‡}) and clockwise (right, **10BC**^{+‡}) structures. Distances are given in Å.

Table 1. Internal and Free Energies of B and C Isomers and of TS NHC Rotational Clockwise (**BC**^{+‡}) and Counterclockwise (**BC**^{-‡}) Barriers in the Gas Phase and Benzene Related to Isomer **B**^a

structure	E_{gas}	G_{gas}	E_{benzene}	G_{benzene}
B	0	0	0	0
C	2.8	3.3	2.4	2.9
BC ^{-‡}	16.0	16.7	15.7	16.4
BC ^{+‡}	16.5	17.9	16.5	18.0

^aEnergies are in kcal/mol.

between the above phenyl group and the chloride (see **10BC**^{+‡} in Figure 2). Differently, the same methyl in the counterclockwise rotation TS (**10BC**^{-‡} in Figure 2) keeps longer distances from the closest phenyl group and the alkylidene carbon.

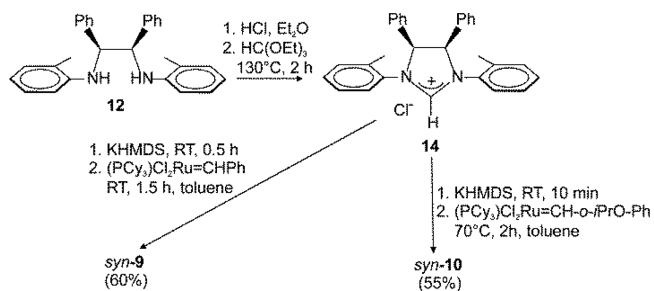
The slight difference of only 0.9 kcal/mol between the calculated lowest TS rotational barrier in benzene (16.4 kcal/mol) and the experimental value (17.3 kcal/mol), corresponding to the **10B** → **10C** direct travel, supports the hypothesis that the observed exchange of isomers **10B** and **10C** occurs through NHC rotation around the C–Ru bond.

The evaluated NHC rotation barrier is lower than barriers measured on Grubbs second-generation catalysts with both *N*-aryl as well as *N*-alkyl substituents.^{8a,13} Indeed, for complex **3** the NHC rotation barrier was estimated to be 21.8 kcal/mol,^{13a,b} whereas for NHC–Ru complexes bearing *N*-phenylethyl groups rotation barriers of about 20–21 kcal/mol were calculated.^{8a} A decrease of rotation barrier was observed only in the case of an unsymmetrical NHC bearing *N*-fluorophenyl *N*-mesityl substituents^{13b} down to 17.9 kcal/mol. Complex **10B** differs from the already investigated catalysts in being a phosphine-free catalyst and presenting backbone substitution and mono-ortho *N*-aryl substituents. The presence of an oxygen in place of a phosphine in a position trans with respect to the NHC should increase the π back-donation from the metal to the NHC, increasing the rotation barrier, as also shown by Thiele et al. investigating Ru bis-NHC complexes with NHC ligand bearing different electron-withdrawing groups.¹⁴ In principle, the inductive electronic donation effect of phenyls on the backbone of **10B** should also increase the barrier, by increasing σ donation and, as a consequence, the π back-donation from the metal to the NHC. In contrast, complex **10B** shows a lower barrier, possibly due to the minor steric hindrance of mono-ortho *N*-aryl groups

in comparison to diortho substitution. Furthermore, it was recently shown by Cavallo et al.¹⁵ that direct electronic donation can be observed by DFT calculations from the C_{ipso} of the *N*-aryl substituents on one side directly to the metal and on the other side to the alkylidene group when correctly oriented. As for complex **10B**, we can expect scarce interaction with the alkylidene due to the orientation characteristic of Hoveyda type complexes as well as, on the other side, labile interaction with the metal due to the *N*-aryl orientation induced by phenyl groups on the backbone. Such minor NHC–metal interactions with respect to Grubbs second-generation complexes could be also responsible for the decreased barrier.

In an attempt to obtain complex **9** in more satisfactory yields, we decided to exploit an alternative route previously reported in the literature.¹⁶ Diamine **12** was converted to imidazolidinium salt **14** by condensation with triethyl orthoformate. This salt was deprotonated in situ by treatment with potassium hexamethyldisilazide (KHMDs) and then mixed with Grubbs I (**1**) in toluene at room temperature to selectively afford the most active isomer, *syn*-**9**, in 60% yield (see Scheme 2). This result was rather

Scheme 2. Synthesis of Complexes *syn*-**9** and *syn*-**10**



unexpected and seems to indicate an important role of the base ($(CF_3)_2CH_3COK$ or KHMDs) which reacts with the NHC ligand precursor to determine the selectivity of the synthesis reaction. A similar protocol was explored also for the preparation of the phosphine-free complex **10** (Scheme 2).^{7d} Again, direct reaction of the imidazolidinium salt with KHMDs and then with Hoveyda–Grubbs II (**2**) at 70 °C led selectively to the isomer *syn*-**10** in 55% yield.

In light of the catalysis results, the possibility of obtaining exclusively the most active *syn* isomers assumes particular relevance. Indeed, the ease of synthesis of stable catalysts plays an important role in determining the feasibility of large-scale industrial applications.

Ring-Closing Metathesis (RCM) Activity. The catalytic behavior of **9** and **10** was first investigated in the RCM reactions of diethyl diallylmalonate (**15**) and diallyl tosylamine (**16**) by monitoring the conversion of each substrate to product via ¹H NMR spectroscopy. For comparison, parallel reactions were performed with the commercial benchmark catalysts **GII-tol**¹⁷ and **HGII-tol**.¹⁸ As clearly shown by the kinetic plots of the RCM of **15** and **16** (Figure 3), catalysts *syn*-**9** and *syn*-**10** were both highly efficient in these cyclization reactions, performing better than their *anti* analogues. The monophosphine complex *syn*-**9** displayed a markedly higher initial reaction rate with respect to its congener *anti*-**9** in both of the ring-closure reactions (Figure 3A,C). Indeed, *syn*-**9** required 30 min to give **17** in more than 98% conversion and 25 min to quantitatively afford **18**, whereas *anti*-**9** was not able to complete the cyclization reactions of both **15** and **16** within 60 min (70% and 90% conversions, respectively).

Consistent with previous results,^{8b} the phosphine-free complexes *syn*- and *anti*-**10** were found to be slow to initiate

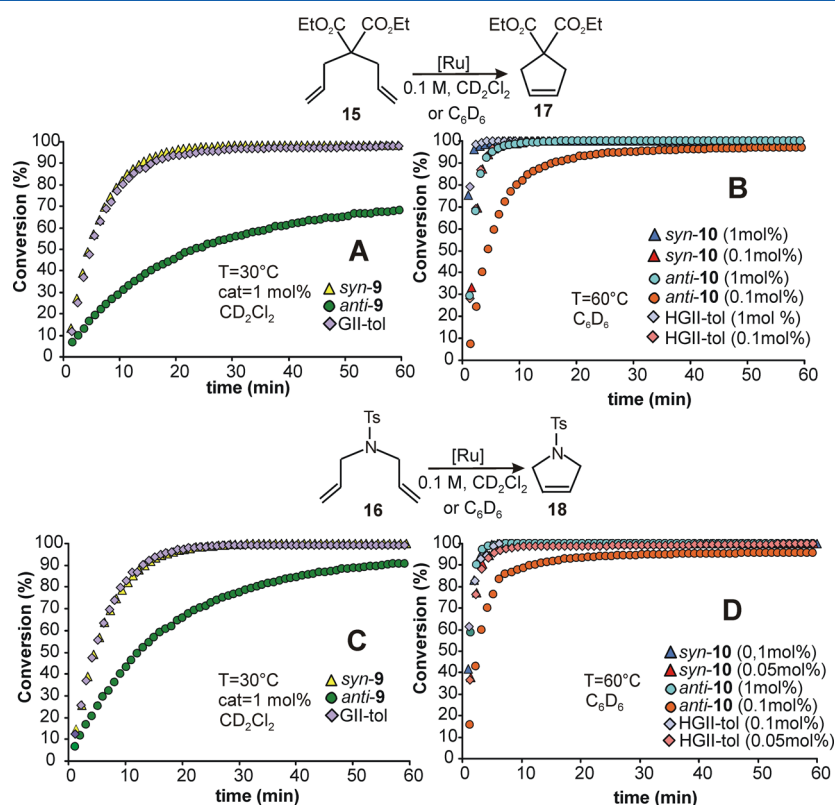


Figure 3. RCM conversion of (A, B) **15** and (C, D) **16**.

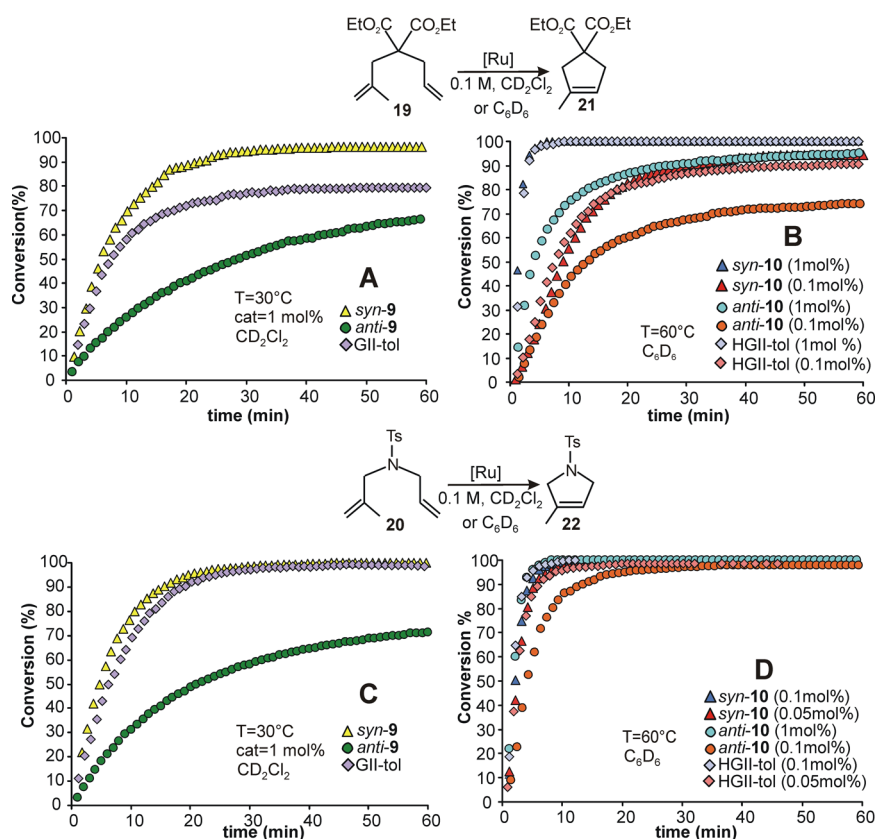


Figure 4. RCM conversion of (A, B) **19** and (C, D) **20**.

RCM reactions under the catalytic conditions (30 °C, CD_2Cl_2) employed for the corresponding monophosphine complexes *syn*- and *anti*-**9** (30 °C, CD_2Cl_2).¹⁹ Therefore, to promote their activation, all of the examined RCM reactions were performed at 60 °C in C_6D_6 . The plots reported in Figure 3B,D showed that *syn*- and *anti*-**10** were both able to promote the RCM of **15** and **16**, with *syn*-**10** behaving as **HGII-tol**. Also in this case, different conformations of the NHC ligand imply different reactivities of the corresponding ruthenium complexes. At a catalyst loading of 1 mol % complete conversion of **15** was obtained with both *syn*-**10** and *anti*-**10** in 5 and 12 min, respectively. When the amount of precatalyst was reduced by 1 order of magnitude (0.1 mol %), *syn*-**10** was able to promote quantitative cyclization of **15** within 30 min, whereas *anti*-**10** needed 60 min to nearly complete the same reaction (97% conversion) (Figure 3B). Lower catalyst loadings employed to perform the RCM of tosylamine **16** allowed us to observe a significant difference between catalyst activities. Indeed, as emerges from the kinetic data of Figure 3D, **16** was efficiently transformed to product **18** (>99% conversion) in only 7 min using 0.05 mol % of *syn*-**10**, whereas precatalyst *anti*-**10** effected complete cyclization to product **18** in 5 min at higher catalyst loading (1 mol %). Moreover, in the same RCM reaction the latter complex was not able to overcome 94% conversion within 60 min at a 10 times lower catalyst loading (0.1 mol %).

The comparison of the catalytic behavior of the *syn* and *anti* conformers of **9** and **10** was then extended to the RCM of slightly hindered malonate (**19**) and tosylamine derivatives (**20**). The kinetic profiles of these experiments and of those performed with **GII-tol** and **HGII-tol** are presented in Figure 4. Similar to the RCM of **15** and **16**, the *syn* complexes **9** and **10** showed higher activity than their *anti* congeners. Moreover, in both trans-

formations *syn*-**9** gave better performances than the commercial catalyst **GII-tol**. The increased steric hindrance of these RCM transformations results in slower reaction rates and highlights more clearly reactivity differences between the two isomeric complexes. It is worth noting that, for the tosylamine derivative **20**, a catalyst loading of 0.05 mol % of *syn*-**10** allowed complete conversion in 14 min (Figure 4D).

Our attention next focused on the challenging RCM of hindered dienes **23** and **24** (Figure 5). Figure 5A shows the results for the RCM of the most sterically demanding malonate derivative **23** promoted by *syn*-**9** and *anti*-**9**. For comparison, the plots of two other efficient *N*-tosyl catalysts for encumbered olefins, such as **5a** and the commercially available **GII-tol**, are also reported. Compound *syn*-**9** not only clearly outperformed *anti*-**9** but was also found to be more efficient than complexes **5a** and **GII-tol**, reaching 92% conversion within 30 min. The latter represents the best result achieved in the RCM of **23** with a monophosphine Ru catalyst up to now. It should be noted that complexes **5a** and **GII-tol** exist as a mixture of inseparable *syn* and *anti* NHC conformational isomers,^{5a,8a,9} and this feature accounts for their lower activity in contrast to *syn*-**9**, consisting of solely *syn*-NHC conformation, which is the spatial arrangement beneficial for the RCM of challenging substrates.^{8,9}

We also performed the RCM of **23** with the chiral monophosphine Ru complex bearing an NHC with *anti* phenyl groups on the backbone and *o*-tolyl *N*-substituents (**GII-C2**),²⁰ which is supposed to preferentially assume the *anti* conformation.²¹ The activity of this complex was comparable to that of complex *anti*-**9** (32% vs 46% conversion, see Figure 5A), providing further confirmation of the relevance of the correct *N*-aryl orientation to successfully perform RCM reactions. The slightly lower difference in activity of **GII-C2** with respect to *anti*-

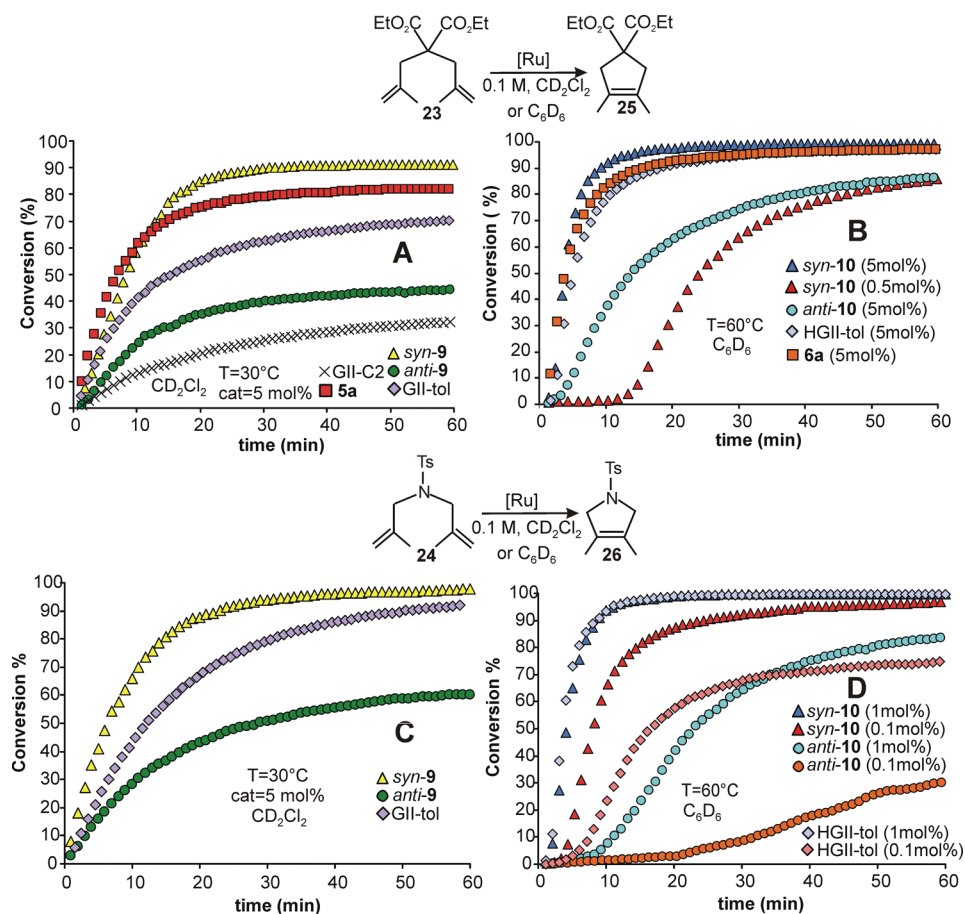


Figure 5. RCM conversion of (A, B) **23** and (C, D) **24**.

9 should arise from the symmetry of the NHC backbone configuration, which has already been shown to be a key element in the ruthenium-catalyzed RCM of olefins.^{8b}

The results for the RCM of **23** to form the tetrasubstituted **25** ring, promoted by phosphine-free catalysts *syn-10*, *anti-10*, **6a**, and commercially available **HGII-tol** are depicted in Figure 5B. Although the differences in overall activity were less evident than for the corresponding phosphine-containing complexes, compound *syn-10* with correctly oriented *N*-tolyl groups showed the highest activity, emerging as one of the most efficient catalysts in the RCM of challenging diolefins. In addition, *syn-10* allowed the formation of tetrasubstituted olefin **25** at a catalyst loading as low as 0.5 mol %, leading to almost full conversion (>96%) within 3 h. The graphs depicted in Figure 5B display that *syn-10*, with one-tenth the catalyst loading, was able to reach the same conversion of *anti-10* (86%) within 60 min, despite the striking difference in their initial rates (a pronounced induction period is indeed observed using 0.5 mol % of *syn-10*). This experimental evidence underlines once again the high efficiency of the *syn* conformer with respect to the *anti* conformer.

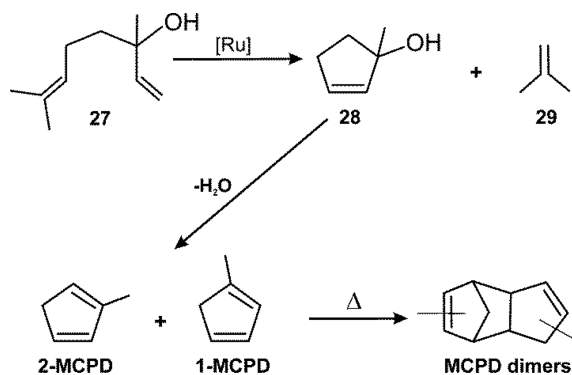
A lower catalyst loading was employed to perform the RCM of the sterically hindered tosylamine substrate **24** in comparison to the malonate analogue **23** (Figure 5C,D). The general reactivity trend is in line with that of previous RCM reactions performed in the presence of the *syn* and *anti* isomers of **9** and **10**. Notably, a nearly quantitative yield (97% in 60 min) was registered at 0.1 mol % of *syn-10* for the most difficult tosylamine derivative **24**, whereas under the same reaction conditions **HGII-tol** reached

75% conversion and *anti-10* just provided 31% conversion (Figure 5D).

The influence of the NHC conformation of **9** and **10** was studied in the RCM of (\pm)-linalool (**27**), a naturally occurring linear terpene alcohol. The skeleton of this diene is particularly intriguing because it is characterized by one monosubstituted and one trisubstituted double bond and bears a methyl substituent on the allylic carbon. Despite the significant steric deactivation, the RCM of **27** has proven to be facilitated by the interaction of the allylic hydroxyl group with the catalytic center,²² resulting in the formation of 1-methylcyclopent-2-en-1-ol (**28**) and isobutylene (**29**) (see Scheme 3). Both of these products represent valuable starting materials for the synthesis of polymers and renewable fuels.^{23–26}

As depicted in Figure 6A, the monophosphine catalysts *syn-9* and *anti-9* efficiently catalyzed the ring closing of **27** at a loading of 1 mol %. For comparison, the plot of the same reaction carried out with the *N*-tolyl catalyst **GII-tol** is also reported. The RCM reactivity trend confirms the superior performance of the *syn* isomer, which reached full conversion in only 7 min (*anti-9* and **GII-tol** required 10 and 13 min, respectively). When the catalyst amount was decreased to 0.1 mol % (Figure 6B), conversion of **27** was incomplete, ranging between 33% (*anti-9*) and 59% (*syn-9*) within 60 min. Prolonged reaction times (48 h) did not significantly improve the yields (for *anti-9* it reached 37%); however, after this time, the complete and spontaneous conversion of the so-formed cyclic alcohol **28** to dehydration products was unexpectedly observed, while the amount of unreacted linalool **27** was found to remain unchanged. In

Scheme 3. Products Derived from the RCM of 27 Promoted by 9 and 10



particular, a complex mixture of 27, 2-methylcyclopentadiene (2-MCPD), and 1-methylcyclopentadiene (1-MCPD) was obtained (Scheme 3). Although RCM reactions of 27 promoted by ruthenium catalysts under dilute conditions have already been reported in the literature,^{7f,27} the authors did not make mention of a similar evolution of the RCM product 28.

To gain more insight into this interesting dehydration process, the fate of the alcohol 28, quantitatively obtained in the RCM reactions conducted at 1 mol % of catalyst, was monitored for longer periods of time. About 5 min after the completion of the RCM reactions promoted by catalysts *syn*-9, *anti*-9, and **GII-tol**, the ¹H NMR signals due to the formation of 2-MCPD began to be visible and within 2 h the RCM product 28 was totally converted into 2-MCPD and a small amount of 1-MCPD. Indeed, the preferentially formed isomer 2-MCPD underwent slow isomerization to the less favored 1-MCPD, leading in 2 days to a final 2-MCPD/1-MCPD ratio of 57/43 with the isomers of 9 and 65/35 with **GII-tol** (see the Supporting Information).

The RCM of 27 carried out with phosphine-free catalysts *syn*-10 and *anti*-10 is reported in Figure 6C. The catalytic behavior of the two conformers of 10 was compared to that of the commercial benchmark catalyst **HGII-tol**. At 1 mol % of loading, catalysts *syn*-10, *anti*-10, and **HGII-tol** showed the same activity, effecting the quantitative ring closure of 27 in 6 min. A slight difference in reactivity among *syn*-10, *anti*-10, and **HGII-tol** was noted by lowering the catalyst loading to 0.1 mol %, as shown by the graphs of Figure 6D. Once again, the *syn* isomer revealed the highest efficiency (>98% conversion within 60 min). The spontaneous conversion of the alcohol 28 obtained through these latter RCM reactions into dehydration products required longer reaction times. In effect, the initial formation of methylcyclopentadiene isomers was observed after 1 day from the completion of the RCM reaction. After 10 days, a complex reaction mixture of alcohol 28, 2-MCPD, 1-MCPD, and methylcyclopentadiene dimers (MCPD dimers) arising from Diels-Alder cycloadditions was detected (Scheme 3). The formation of MCPD dimers is facilitated by the higher reaction temperature required by phosphine-free catalysts (60 °C), with respect to phosphine-containing complexes, to effectively perform RCM reactions.

Of particular significance is the obtainment of isobutylene and of well-defined mixtures of methylcyclopentadiene isomers from the RCM reactions described above. Indeed, isobutylene can be, for example, polymerized to polyisobutylene,²³ dimerized to produce high-octane gasoline,²⁴ or trimerized to produce jet fuel,²⁵ whereas methylcyclopentadiene isomers can be dimerized and subsequently hydrogenated to give specialized fuel products.²⁶

Recently, Harvey et al. reported on solvent-free RCM reactions of linalool 27 conducted with three commercial Ru-based catalysts (1, 4, and **GII-tol**).²⁸ Among them, at 60 °C, complexes 1 and 4 were found to furnish the cyclic alcohol 28 along with dehydrated products such as cyclopentenol ethers,

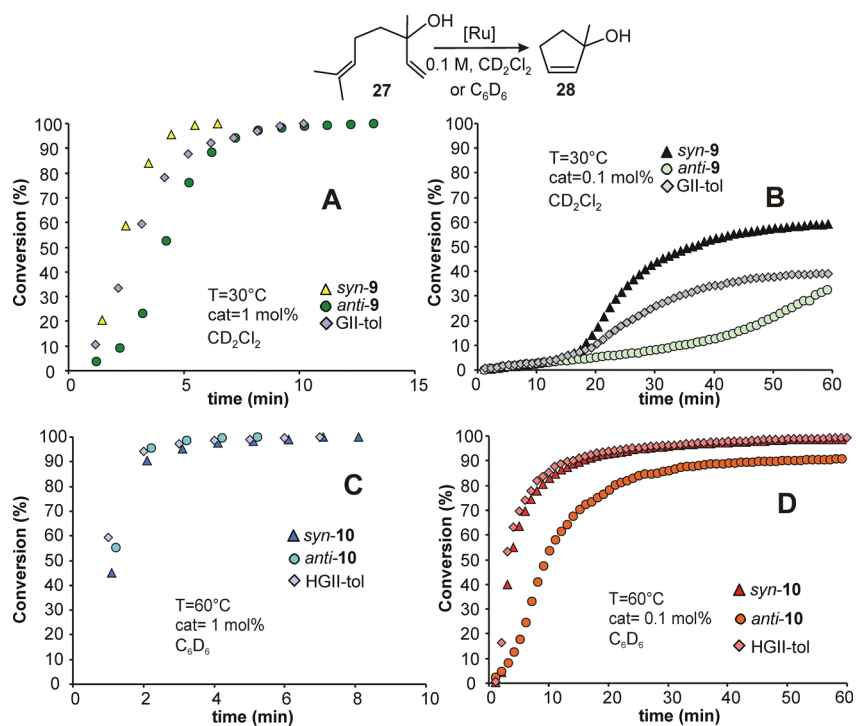


Figure 6. RCM conversion of 27.

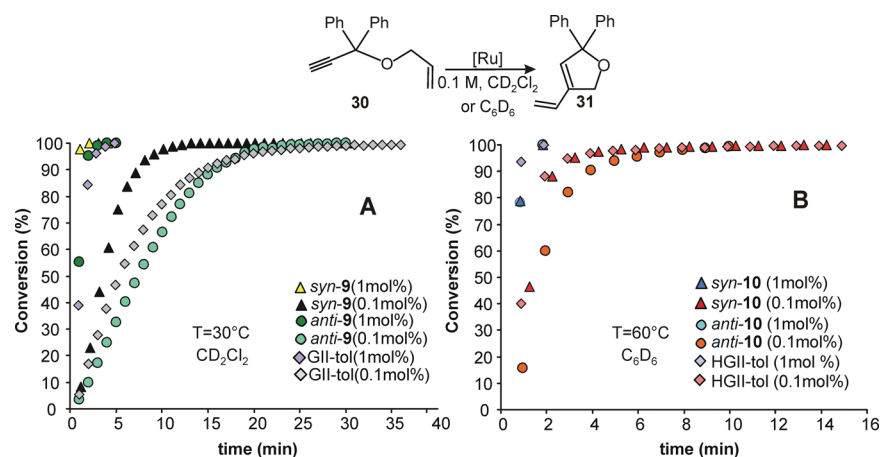


Figure 7. RCM conversion of **30**.

MCPD isomers, and MCPD dimers. This finding was explained by considering **1** and **4** as able to dehydrate a tertiary alcohol. On the other hand, complex **1** was previously found to be able to promote the direct dehydration of an RCM alcohol product.²⁹ By consideration of the nature of the substrate **27**, an alternative interpretation of the experimental data was proposed. Accordingly, the occurrence of a ligand exchange reaction at the ruthenium center of the alkoxy group for chloride would release catalytic amounts of HCl, sufficient to promote the dehydration of the alcohol.²⁸

The dehydration process following the RCM reactions carried out with complexes **9**, **10**, **GII-tol**, and **HGII-tol** appears to be mediated by ruthenium catalyst, possibly by species derived from catalyst decomposition. As a general remark, it is well known that Ru complexes bearing NHCs with reduced bulk at the ortho positions of *N*-aromatic substituents are rather unstable and are susceptible to decomposition through C–H activation processes of the *N*-aryl groups on the NHC ligand.³⁰

The above RCM results clearly indicate that the dehydration process involving the cyclic alcohol **28** is much more favored in the presence of the phosphine-containing catalysts **9** and **GII-tol** with respect to the analogous phosphine-free complexes **10** and **HGII-tol**. Since the PCy₃ ligand released in the reaction mixture after the initial metathesis step is known to contribute to catalyst degradation,^{30a} it is reasonable to suppose that alcohol **28** dehydration observed in the presence of complexes **9** and **GII-tol** could be activated by species arising from decomposition of the catalyst mediated by PCy₃. To support this hypothesis, the RCM of **28** was performed in the presence of the phosphine-free catalyst *syn*-**10** in CD₂Cl₂ at 30 °C. Full conversion of **27** was reached after 4.5 h; however, the reaction mixture was further monitored over the course of 1 week. No dehydration of the product **28** was observed. After this time, an excess of PCy₃ was added to the reaction mixture, and the formation of dehydrated products began to be evident. A mixture of **28** (67%), MCPD isomers (25%), and Diels–Alder adducts (8%) was obtained after 6 days from the addition of PCy₃, thus indicating that the presence of this component in the reaction mixture plays a role in the alcohol dehydration process. Nevertheless, the influence of the phosphine ligand as well as of the nature of the catalyst employed on the composition of the final mixtures of the RCM reaction of **27** is not at all clarified and is still under investigation.

To further explore the catalytic potential of the isomers of **9** and **10** in RCM reactions, ring-closing ene-yne metathesis (RCEYM) was investigated with the standard test substrate **30**

(Figure 7). This class of RCM reactions is a powerful tool in organic synthesis because it allows the atom-economical formation of cyclic functionalized products, usually present in many drugs and natural products. As depicted in Figure 7, both catalysts **9** successfully performed the RCM of **30**, as did the benchmark catalyst **GII-tol**. At 1 mol %, *syn*-**9** required only 2 min to totally cyclize **30**, whereas *anti*-**9** and **GII-tol** needed 4 and 5 min, respectively (Figure 7A). An appreciable difference in reactivity was detected in the RCM conducted at 0.1 mol %, where the *syn* isomer completed the cyclization in 13 min and the *anti* isomer achieved the same result in 29 min. More than 35 min is required by **GII-tol** to approach full conversion. With the phosphine-free catalysts *syn*- and *anti*-**10**, no difference in activity could be observed between the catalysts at 1 mol % of loading (Figure 7B). Indeed, both complexes converted all the substrate in less than 2 min. The same catalytic behavior was observed for catalyst **HGII-tol**. A small amount of discrimination was instead noticed at 0.1 mol % of catalyst loading; in this case, *syn*-**10** employed only 8 min to quantitatively effect the cyclization (Figure 7B), as did **HGII-tol**. Significantly, the overall reactivity profile in the examined RCEYM reaction puts *syn* conformers of **9** and **10** among the most efficient catalysts known.³¹

Among the RCM transformations, a special place is occupied by macrocyclic RCM reactions.^{1d,3e,32} Indeed, macrocyclic frameworks are commonly found in bioactive natural products and pharmaceutical molecules and their construction by RCM often represents a key step in the synthesis of natural products containing large rings. The most active catalysts *syn*-**9** and *syn*-**10** were therefore tested in the RCM of the diene esters **32** and **33** to form the 14-membered lactones **34** and **35**, respectively (Scheme 4). The reactions were monitored by GC analysis over a period of 24 h, and the best results are reported in Table 2.

In the formation of the 14-membered lactone **34**, *syn*-**9** gave nearly quantitative yields of the RCM product in only 30 min (Table 2, entry 1), showing superior performance with regard to the commercial monophosphine catalysts **2** and **GII-tol** (Table 2, entries 3 and 4). Moreover, *syn*-**9** was found to be more efficient than the analogous catalyst **5a** with methyl groups on the NHC backbone (Table 2, entry 5). The different macro-RCM reactivities observed for *syn*-**9**, **GII-tol**, and **5a** can be related to the different substitution patterns of the NHC backbone. As already reported, the presence of substituents on the NHC backbone improves catalyst stability, because restriction of the rotation of the *N*-aryl groups hinders the necessary proximity of an aryl C–H bond and the ruthenium center to promote

Scheme 4. Macrocylic RCM of 32 and 33

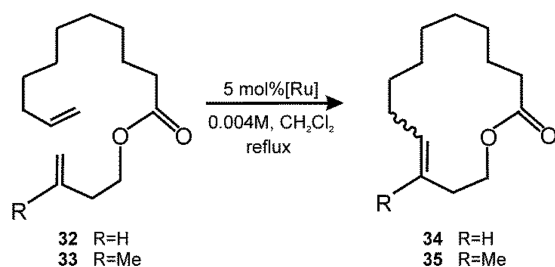


Table 2. Synthesis of Macrocylic Lactones 34 and 35

entry ^a	substrate	catalyst	time (h)	yield (%) ^b	<i>E:Z</i> ^c	<i>E:Z</i> calcd
1	32	<i>syn</i> -9	0.5	96	90:10	
2	32	<i>syn</i> -10	0.5	99	94:6	
3 ^d	32	2	2	97	94:6	96.5:3.5
4 ^d	32	GII-tol	4	54	94:6	
5 ^d	32	Sa	4	73	94:6	
6	33	<i>syn</i> -9	24	76	82:18	
7	33	<i>syn</i> -10	24	47	75:25	85:15 ^e
8 ^f	33	2	40	57	87:13	

^aReactions in CH₂Cl₂ (4 mM) at reflux temperature. ^bIsolated yield. ^c*E:Z* ratios were determined by GC and NMR spectroscopy. ^dGC yield, taken from ref 33. ^e*E:Z* ratios obtained from DFT calculated energies in CH₂Cl₂ (for computational details see the Experimental Section). ^fGC yield, taken from ref 34a.

degradation pathways.^{7a} As a consequence, high activity deriving from correct *syn* *N*-tolyl conformation, combined with increased stability, renders *syn*-9 an excellent catalyst for this macrocyclization. The same result was obtained also in the presence of *syn*-10; nonetheless, it usually requires higher reaction temperatures than the corresponding phosphine-containing complex *syn*-9. The experimentally observed *E:Z* ratios are in good agreement with the calculated *E:Z* populations, indicating a mainly thermodynamically controlled RCM in the formation of 34, for all catalysts.

A more stringent test is the formation of the 14-membered lactone 35, containing a trisubstituted double bond.³⁴ In this reaction, *syn*-9 was revealed as the most efficient catalyst known to date, proving once again its superiority to the commercially available catalyst 2 (Table 2, entry 6). The decreased efficiency of *syn*-10 in the formation of 35 was not too surprising, since increased steric hindrance of the reaction could necessitate higher temperature to improve catalyst performance.³⁵

Molecular modeling of *E* and *Z* isomers of 35 was performed to afford further information on catalyst behaviors. Minimum energy structures of 35-*E* and 35-*Z* are shown in Figure 8. The

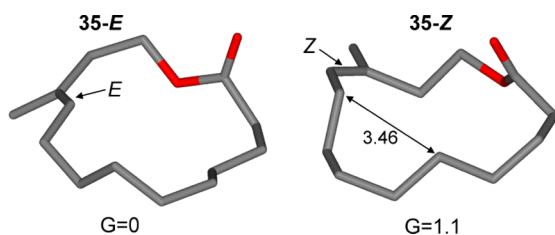


Figure 8. Structures and free energies of the *E* and *Z* isomers of compound 35 calculated in CH₂Cl₂. Energies are in kcal/mol, distances are in Å.

free energy difference calculated in CH₂Cl₂ allowed us to determine the relative thermodynamic stabilities of 35-*E* and 35-*Z*. Indeed, calculated *E:Z* populations are 85% (35-*E*) and 15% (35-*Z*), very close to the experimental ratio obtained by RCM in the presence of catalysts 2, *syn*-9, and *syn*-10. DFT calculations confirm the tendency of the examined catalysts to give products under thermodynamic control.

Ring-Opening Metathesis Polymerization (ROMP) Activity. Afterward, the catalytic behavior of the conformers of 9 and 10 was examined in the ROMP of 1,5-cyclooctadiene (36; COD). Time–conversion studies for the ROMP of 36 in the presence of 0.1 mol % and 0.01 mol % of catalyst are depicted in Figure 9, and the most significant results are summarized in Table 3.

On examination of these data, a remarkable difference in overall activity between phosphine-containing catalysts *syn*-9 and *anti*-9 emerged at both 0.1 and 0.01 mol % (Figure 9A; entries 1, 2, 4 and 5, Table 3). The *syn* orientation of the *N*-tolyl groups on the NHC is revealed once again to be the best orientation to gain high catalyst performance. As for *E:Z* selectivity, no relevant influence could be attributed to the different NHC conformations of *syn*-9 and *anti*-9. *Syn*-9 gave conversions and *E:Z* ratios similar to those for GII-tol^{8a} under identical reaction conditions (entries 3 and 6, Table 3), underlining the negligible role of the phenyl substituents on the NHC backbone in addressing activity and stereoselectivity in the ROMP of COD, as already observed for catalysts Sa and 7a with methyl substituents on the backbone.^{8a}

It should be noted that in the same ROMP reaction no difference in overall activity could be appreciated among the phosphine-free complexes *syn*-10, *anti*-10, and HGII-tol. This could be related to the high temperature required for the activation of this class of catalysts, which, as already observed, tends to even out reactivity differences.

Cross-Metathesis (CM) Activity. Finally, the catalytic performance of *syn*-9 and *anti*-9 was compared in the CM of allyl benzene (37) and *cis*-1,4-diacetoxy-2-butene (38), illustrated in Scheme 5. Both conformers gave high conversions to the desired heterocoupled product 39, with *syn*-9 (91% yield) once again performing better than its *anti* analogue (81% yield). The presence of phenyl groups on the NHC backbone increases catalyst efficiency, as demonstrated by the improved yields observed for complexes 9 with respect to that obtained with the benchmark catalyst GII-tol (60%).^{8a} As for the stereoselectivity, the *E:Z* ratios clearly appear to be not influenced by the NHC conformation and the backbone substitution.

CONCLUSION

In summary, a systematic study on the catalytic behavior of phosphine-containing and phosphine-free NHC ruthenium catalysts incorporating *syn* phenyl groups on the backbone and differently oriented *N*-tolyl groups (*syn* and *anti*) in several metathesis transformations (such as RCM, RCEYM, ROMP, and CM) of representative substrates was reported.

Complexes with frozen *syn* *N*-tolyl groups (*syn*-9 and *syn*-10) were clearly identified as the most efficient in all of the examined reactions, outperforming also the commercial *N*-tolyl catalysts GII-tol and HGII-tol in almost all cases. This finding suggests that the correct orientation of *N*-tolyl rings is a general requirement to successfully accomplish olefin metathesis transformations. As shown for the RCM of hindered olefins,^{8b} the symmetric tilt of the *N*-tolyl groups induced by the *syn*-phenyl substituents on the NHC backbone leads to a more sterically

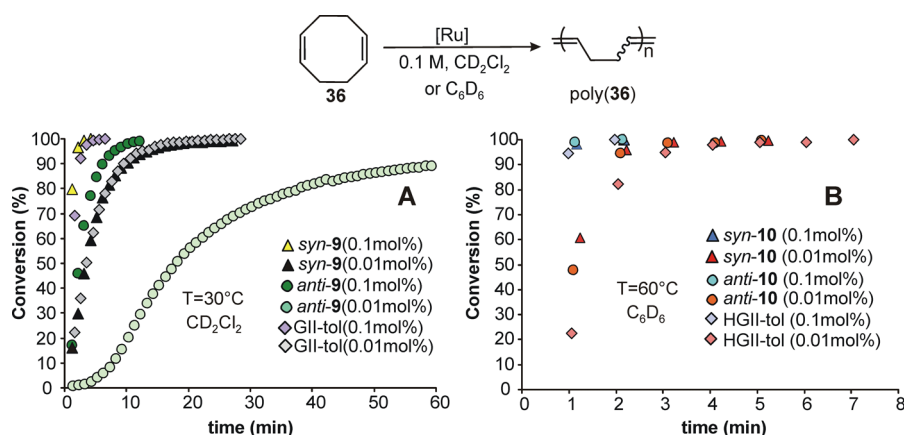


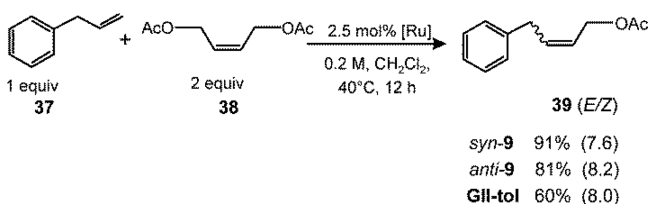
Figure 9. ROMP conversion of 36.

Table 3. ROMP of 36

entry	catalyst	time (min)	poly(36) yield (%) ^a	<i>E:Z</i> ^b
1 ^c	<i>syn</i> -9	3	>99	1.1
2 ^c	<i>anti</i> -9	12	>99	0.8
3 ^c	GII-tol	4	>99	1.3
4 ^d	<i>syn</i> -9	27	>99	0.7
5 ^d	<i>anti</i> -9	60	90	0.4
6 ^d	GII-tol	27	>99	1.0
7 ^e	<i>syn</i> -10	2	>99	2.4
8 ^e	<i>anti</i> -10	2	>99	4.0
9 ^e	HGII-tol	2	>99	3.8
9 ^f	<i>syn</i> -10	5	>99	1.7
10 ^f	<i>anti</i> -10	5	>99	2.6
11 ^f	HGII-tol	6	>99	2.7

^aDetermined by ¹H NMR. ^b*E/Z* ratios were determined by ¹H and ¹³C NMR of isolated products. ^cConditions: reactions in CH₂Cl₂, at 30 °C, catalyst 0.1 mol %. ^dConditions: reactions in CH₂Cl₂, at 30 °C, catalyst 0.01 mol %. ^eConditions: reactions in C₆D₆, at 60 °C, catalyst 0.1 mol %. ^fConditions: reactions in C₆D₆, at 60 °C, catalyst 0.01 mol %.

Scheme 5. CM of Substrates 37 and 38



open space around the ruthenium. Very likely, this feature also clears the way to the easy approach and reaction of different metathesis substrates. This insight can contribute to inspire further ligand design and modification strategies in order to improve olefin metathesis ruthenium catalyst efficiency.

To render the most performing *syn* catalysts really attractive for large-scale applications, more convenient and straightforward syntheses of *syn*-9 and *syn*-10 were also reported. In particular, *syn*-9 was selectively obtained in good yield, free from the less active *anti* conformer without requiring chromatographic purification.

An unexpected result with interesting implications is related to the involvement of *syn* and *anti* *N*-tolyl catalysts, as well as of commercial GII-tol, in the dehydration reaction of the 1-methylcyclopent-2-en-1-ol (28) produced by the RCM of linalool

(27). Indeed, this process leads to an exceptionally well-defined distribution of methylcyclopentadiene isomers (2-MCPD and 1-MCPD), which represent a viable route to specialized fuel products. Work is in progress in order to rationalize the behavior of *N*-tolyl catalysts in mediating the dehydration of the alcohol.

EXPERIMENTAL SECTION

Synthesis of Imidazolium Chloride 14. A diethyl ether solution of 12 was treated with a solution of hydrogen chloride (2.0 M in diethyl ether) to precipitate the diamine hydrochloride salt as an off-white powder. The product was collected by filtration and washed with diethyl ether. The diamine salt (1.94 mmol, 902 mg) and a large excess of triethyl orthoformate (3.3 mL) was placed in a 50 mL round-bottom flask equipped with a magnetic stirrer. The flask was fitted with a condenser and heated to 135 °C in an oil bath for 2 h. When it was cooled to room temperature, the solid product was washed several times with hexane and then with Et₂O to give the desired imidazolium chloride salt 14 as a pale yellow solid (1.52 mmol, 668 mg, 78.4% yield).

¹H NMR (250 MHz, CD₃CN): δ 9.41 (br s, 1H, NCHN); 7.52 (br s, 2H); 7.36–7.26 (br m, 6H); 7.14–7.10 (br m, 10H); 6.73 (br s, 2H, N-CH(Ph)CH(Ph)-N), 2.6 (br s, 6H, PhCH₃). ¹³C NMR (62.5 MHz, CD₂Cl₂): δ 161.1 (NCN), 133.9, 133.4, 132.4, 131.7, 130.0, 129.7, 128.6, 128.6, 127.9, 127.5, 72.3 (N-CH(Ph)CH(Ph)-N), 20.0 (Ph-CH₃). ESI⁺ MS: *m/z* 403.1 [M + (Cl⁻)].

Synthesis of Ru Complex *syn*-9. In a glovebox, a 10 mL Schlenk tube was charged with imidazolium salt 14 (0.341 mmol, 150 mg), potassium hexamethyldisilazide (KHMDS; 0.341 mmol, 0.68 mL, 0.5 M in toluene), and (PCy₃)₂Ru(=CHPh)Cl₂ (0.227 mmol, 186 mg) dissolved in 2 mL of toluene. The reaction mixture was stirred at room temperature for 1 h; then toluene was evaporated under vacuum and a small amount of MeOH was added with stirring. The precipitate was filtered off, washed with MeOH, and dried in vacuo. The desired complex *syn*-9 was obtained as a brown powder (0.136 mmol, 128 mg, 60%).

¹H NMR (400 MHz, C₆D₆): δ 19.83 (br s, 1H, Ru=CHPh); 9.07 (d, ³J_{H-H} = 7.67 Hz; 1H); 7.22 (t, 1H); 6.96 (m, 6H); 6.87 (t, 2H); 6.80 (t, 3H), 6.75–6.64 (overlapped m, 6H); 6.41 (t, ³J_{H-H} = 7.28 Hz; 2H); 5.98 (d, ³J_{H-H} = 10.03 Hz; 2H); 5.45 (br d, 2H, N-CH(Ph)CH(Ph)-N); 2.78 (s, 6H, Ph-CH₃); 2.24–1.0 (33H). ¹³C NMR (100 MHz, C₆D₆): δ 299.4 (br s, Ru=CHPh); 222.3 (*i*NCN, ²J_{C-P} = 65.82 Hz); 151.1; 139.6; 138.6; 137.5; 136.1; 133.8; 133.1; 131.9; 130.3; 129.7; 129.5; 128.82; 125.9; 73.9 (N-CH(Ph)CH(Ph)-N); 73.2 (N-CH(Ph)CH(Ph)-N); 33.1; 33.0; 29.1; 28.0; 26.7; 20.8 (Ph-CH₃); 19.3 (Ph-CH₃). ³¹P NMR (161.97 MHz, C₆D₆): δ 22.8. Anal. Calcd for C₃₄H₆₅Cl₂N₂PRu (944.33): C, 68.63; H, 6.93; N, 2.96. Found: C, 69.15; H, 6.98; N, 2.99.

Synthesis of *syn*-10. In a glovebox, to a suspension of 14 (0.752 mmol, 330 mg) in toluene was added KHMDS (0.827 mmol, 165 mg). The reaction mixture was stirred for 15 min at room temperature, and then (PCy₃)₂Ru(=CH-*o*-iPrC₆H₄)Cl₂ (0.399 mmol, 239 mg) was added. The flask was removed from the glovebox, and the contents were

stirred at 70 °C for 3.0 h. The reaction mixture was cooled to room temperature and purified by column chromatography on TSI silica gel (*n*-hexane/diethyl ether 2/1 to 1/1). The solvent was removed in vacuo to give **syn-10** as a green powder (0.179 mmol, 129 mg, 45.0%). Crystals suitable for X-ray analysis were grown by vapor diffusion of pentane into a concentrated benzene solution of the complex at room temperature.

¹H NMR (400 MHz, CD₂Cl₂): δ 16.22 (s, 1H, Ru=CH-*o*-OiPrC₆H₄); 8.78 (d, 1H, ³J_{H-H} = 7.64 Hz); 7.57 (t, 1 H); 7.54 (d, 1 H, ³J_{H-H} = 7.90 Hz); 7.42–7.35 (m, 2H); 7.27–7.24 (m, 2H); 7.17–7.14 (m, 4H); 7.09–7.02 (m, 6H); 7.00–6.90 (m, 2H); 6.86–6.84 (m, 1H); 6.03 (d, 2H, ³J_{H-H} = 9.96 Hz); 5.93 (d, 2H, ³J_{H-H} = 9.96 Hz, N-CH(Ph)CH(Ph)-N); 5.02 (q, 1H, ³J_{H-H} = 6.15 Hz, CH(CH₃)₂); 2.66 (s, 3H, Ph-CH₃); 2.56 (s, 3H, Ph-CH₃); 1.54 (d, 3H, ³J_{H-H} = 6.15 Hz, CH(CH₃)₂); 1.33 (d, 3H, ³J_{H-H} = 6.15 Hz, CH(CH₃)₂). ¹³C NMR (75 MHz, C₆D₆): δ 294.4 (Ru=CH-*o*-OiPrC₆H₄); 215.3 (iNCN); 153.3; 144.6; 141.3; 140.6; 138.0; 137.5; 133.8; 132.2; 131.2; 130.8; 129.5; 122.34; 113.3; 75.0 (N-CH(Ph)CH(Ph)-N); 74.3 (N-CH(Ph)CH(Ph)-N); 72.6 (CH(CH₃)₂); 22.4 (Ph-CH₃); 22.0 (Ph-CH₃); 20.6 (CH(CH₃)₂); 18.9 (CH(CH₃)₂). Anal. Calcd for C₃₉H₃₈Cl₂N₂O₄Ru: C, 64.81; H, 5.30; N, 3.88. Found C, 64.80; H, 5.27; N, 3.85.

General Procedures for RCM Reactions. An NMR tube with a screw-cap septum top was charged with 0.80 mL of a CD₂Cl₂ or C₆D₆ solution of catalyst (0.05–5%). After equilibration at the appropriate temperature (30 °C for the reaction in CD₂Cl₂, 60 °C for the reaction in C₆D₆) of the sample in the NMR probe, 0.080 mmol of substrate was injected into the tube (0.1 M substrate/solvent ratio). Conversions of each substrate to product were monitored over time by ¹H NMR.

RCM of Diethyl Diallylmalonate (15) (Figure 3). A 19.5 μL portion (0.080 mmol) of **15** was injected into a heated NMR tube containing 0.80 mL of catalyst solution (0.1–1 mol %), and the conversion to **17** was determined by integrating the methylene protons in the starting material, δ 2.61 (dt) in CD₂Cl₂ or 2.84 (dt) in C₆D₆, and those in the product, δ 2.98 (s) in CD₂Cl₂ or 3.14 (s) in C₆D₆.

RCM of *N*-Tosyldiallylamine (16) (Figure 3). A 17.2 μL portion (0.080 mmol) of **16** was injected into a heated NMR tube containing 0.80 mL of catalyst solution (0.05–1 mol %), and the conversion to **18** was determined by integrating the methylene protons in the starting monomer, δ 3.70 (dt) in CD₂Cl₂ or 3.71 (d) in C₆D₆, and those in the product, δ 4.00 (s) in CD₂Cl₂ or 3.90 (s) in C₆D₆.

RCM of Diethyl Allylmethylmalonate (19) (Figure 4). A 20.5 μL portion (0.080 mmol) of **19** was injected into the heated NMR tube containing 0.80 mL of catalyst solution (0.1–1 mol %), and the conversion to **21** was determined by integrating the methylene protons in the starting material, δ 2.67 (s), 2.64 (dt) in CD₂Cl₂ or 2.96 (d), 2.93 (s) in C₆D₆, and those in the product, δ 2.93 (s), 2.88 (m) in CD₂Cl₂ or 3.18 (m), 3.07 (s) in C₆D₆.

RCM of *N*-tosylallylmethylamine (20) (Figure 4). A 19.4 μL portion (0.080 mmol) of **20** was injected into a heated NMR tube containing 0.80 mL of catalyst solution (0.05–1 mol %), and the conversion to **22** was determined by integrating the methylene protons in the starting material, δ 3.63 (s), 2.64 (dt) in CD₂Cl₂ or 3.70 (d), 3.67 (s) in C₆D₆, and those in the product, δ 3.91 (s), 2.88 (m) in CD₂Cl₂ or 3.96 (m), 3.82 (s) in C₆D₆.

RCM of Diethyl Dimethylmalonate (23) (Figure 5). A 21.6 μL portion (0.080 mmol) of **23** was injected into a heated NMR tube containing 0.80 mL of catalyst solution (0.5–5 mol %) and the conversion to **25** was determined by integrating the methylene protons in the starting material, δ 2.71 (s) in CD₂Cl₂ or 2.98 (s) in C₆D₆, and those in the product, δ 2.89 (s) in CD₂Cl₂ or 3.15 (s) in C₆D₆.

RCM of *N*-Tosyldimethylamine (24) (Figure 5). A 20.2 μL portion (0.080 mmol) of **24** was injected into a heated NMR tube containing 0.80 mL of catalyst solution (0.1–1 mol %), and the conversion to **26** was determined by integrating the methylene protons in the starting material, δ 3.61 (s) in CD₂Cl₂ or 3.69 (s) in C₆D₆, and those in the product, δ 3.87 (s) in CD₂Cl₂ or 3.90 (s) in C₆D₆.

RCM of (±)-Linalool (27) (Figure 6). A 14.3 μL portion (0.080 mmol) of **27** was injected into a heated NMR tube containing 0.80 mL of catalyst solution (0.1–1 mol %), and the conversion to **28** was determined by integrating the methyl protons in the starting material, δ

1.25 (s) in CD₂Cl₂ or 1.13 (br s) in C₆D₆, and those in the product, δ 1.35 (s) in CD₂Cl₂ or 1.26 (br s) in C₆D₆.

RCEYM of (1-(Allyloxy)prop-2-yn-1,1-diyl)dibenzene (30) (Figure 7). Runs at 1 mol %. An NMR tube with a screw-cap septum top was charged with 0.750 mL of a CD₂Cl₂ or C₆D₆ solution of **30** (21.3 mg, 0.080 mmol). After equilibration at the appropriate temperature of the sample in the NMR probe, 50 μL of a 0.016 M solution of catalyst was injected into the tube. The reaction was monitored as a function of time, and the conversion to **31** was determined by integrating the methylene protons in the starting material, δ 4.03 (m) in CD₂Cl₂ or 4.11 (m) in C₆D₆, and those in the product, δ 4.75 (m) in CD₂Cl₂ or 4.50 (m) in C₆D₆.

Runs at 0.1 mol %. An NMR tube with a screw-cap septum top was charged with 0.80 mL of a CD₂Cl₂ or C₆D₆ solution of **30** (21.3 mg, 0.080 mmol). After equilibration at the appropriate temperature of the sample in the NMR probe, the reaction was started, with injection of 5 μL of a 0.016 M catalyst solution.

Macrocyclic RCM of Diene Esters 32 and 33 (Table 2). A 100 mL three-neck round-bottom flask was fitted with a condenser and two additional funnels. Solutions of the ruthenium carbene (6.0 μmol) and of the appropriate diene (**32** or **33**) (120 μmol), each in 10 mL of CH₂Cl₂, were independently added dropwise to refluxing CH₂Cl₂ (10 mL) over a period of 15 min under nitrogen. Aliquots were removed periodically for GC analysis, and GC retention times and integrations were confirmed with samples of authentic material. After 24 h, the solvent was removed in vacuo and the residue purified by flash chromatography to afford analytically pure compounds.

ROMP of COD (36) (Figure 9, Table 3). Procedures are as described for RCM reactions. A 49.1 μL portion (0.40 mmol) of **36** was injected into the heated NMR tube containing 0.80 mL of catalyst solution (0.01–0.1 mol %), and the conversion to poly(**36**) was determined by integrating the methylene protons in the starting monomer, δ 2.36 (m) in CD₂Cl₂ or 2.22 (m) in C₆D₆, and those in the product, δ 2.09 (br m)–2.04 (br m) in CD₂Cl₂ or 2.14 (br m)–2.10 (br m) in CD₂Cl₂ in C₆D₆.

CM of Allylbenzene (37) and *cis*-(1,4)-Diacetoxy-2-butene (38) (Scheme 5). In an oven-dried 4 mL vial (equipped with a magnetic stirrer) were added simultaneously a 33 μL amount of **37** (0.25 mmol) and 80 μL of **38** (0.5 mmol) via syringe to a stirred solution of the catalyst (0.0065 mmol) in 1.25 mL of CH₂Cl₂. The mixture was allowed to react for 12 h at 40 °C. The reaction mixture was concentrated and purified directly on a silica gel column (9/1 hexane/ethyl acetate). **39** was obtained as a pale oil. The *E:Z* ratio was determined by integration of peaks at δ 4.73 and 4.55 (CDCl₃).

■ ASSOCIATED CONTENT

Supporting Information

Text, figures, and an xyz file giving additional experimental details, detailed NMR spectra, and Cartesian coordinates for the optimized structures. This material is available free of charge via the Internet at <http://pubs.acs.org>.

■ AUTHOR INFORMATION

Corresponding Author

*E-mail for F.G.: fgrisi@unisa.it.

Notes

The authors declare no competing financial interest.

■ ACKNOWLEDGMENTS

This paper is dedicated to Professor Adolfo Zambelli on the occasion of his 80th birthday. The authors thank Dr. Patrizia Iannece and Patrizia Oliva for technical assistance. Computational support from CINECA-High Performance Computing Portal in the framework of a class C awarded proposal to the ISCRA programme (code RCMMSMO - HP10C8VOGT) and financial support from the Ministero dell'Università e della Ricerca Scientifica e Tecnologica are gratefully acknowledged.

REFERENCES

- (1) (a) Chauvin, Y. *Angew. Chem.* **2006**, *118*, 3824; *Angew. Chem., Int. Ed.* **2006**, *45*, 3740–3747. (b) Schrock, R. R. *Angew. Chem.* **2006**, *118*, 3832; *Angew. Chem., Int. Ed.* **2006**, *45*, 3748–3759. (c) Grubbs, R. H. *Angew. Chem.* **2006**, *118*, 3845; *Angew. Chem., Int. Ed.* **2006**, *45*, 3760–3765. (d) Grubbs, R. H. *Handbook of Metathesis*; Wiley-VCH: Weinheim, Germany, 2003; Vols. 1–3. (e) Connon, S. J.; Blechert, S. In *Ruthenium Catalysts and Fine Chemistry*; Dixneuf, P. H., Bruneau, C., Eds.; Springer: Heidelberg, Germany, 2004; Vol. 11, p 93. (f) Fürstner, A. *Angew. Chem.* **2000**, *112*, 3140–3172; *Angew. Chem., Int. Ed.* **2000**, *39*, 3012–3043. (g) Hoveyda, A. H.; Zhugralin, A. R. *Nature* **2007**, *450*, 243–251. (h) Deshmukh, P. H.; Blechert, S. *Dalton Trans.* **2007**, 2479–2491. (i) Astruc, D. *New J. Chem.* **2005**, *29*, 42–56. (j) Lozano-Vila, A. M.; Monsaert, S.; Bajek, A.; Verpoort, F. *Chem. Rev.* **2010**, *110*, 4865–4909.
- (2) (a) Vougioukalakis, G. C.; Grubbs, R. H. *Chem. Rev.* **2010**, *110*, 1746–1787. (b) Samojlowicz, C.; Bieniek, M.; Grela, K. *Chem. Rev.* **2009**, *109*, 3708–3742. (c) Diesendruck, C. E.; Tzur, E.; Lemcoff, N. G. *Eur. J. Inorg. Chem.* **2009**, 4185–4203. (d) Fischmeister, C.; Dixneuf, P. H. *Metathesis Chemistry: From Nanostructure Design to Synthesis of Advanced Materials*; Imamoglu, Y., Dragutan, V., Eds.; Springer: Dordrecht, The Netherlands, 2007; pp 3–27. (e) Bieniek, M.; Michrowska, A.; Usanov, D. L.; Grela, K. *Chem. Eur. J.* **2008**, *14*, 806–818.
- (3) (a) Bielawski, C. W.; Grubbs, R. H. *Prog. Polym. Sci.* **2007**, *32*, 1–29. (b) Frenzel, U.; Nuyken, O. *J. Polym. Sci., Part A: Polym. Chem.* **2002**, *40*, 2895–2916. (c) Buchmeiser, R. M. *Chem. Rev.* **2000**, *100*, 1565–1604. (d) Leitgeb, A.; Wappel, J.; Slugovc, C. *Polymer* **2010**, *51*, 2927–2946. (e) Gradillas, A.; Pérez-Castells, J. *Angew. Chem.* **2006**, *118*, 6232–6247; *Angew. Chem., Int. Ed.* **2006**, *45*, 6086–6101. (f) Conrad, J. C.; Fogg, D. E. *Curr. Org. Chem.* **2006**, *10*, 185–202. (g) Monfette, S.; Fogg, D. E. *Chem. Rev.* **2009**, *109*, 3783–3816. (h) Nolan, S. P.; Clavier, H. *Chem. Soc. Rev.* **2010**, *39*, 3305–3316. (i) Donohe, T. J.; Fishlock, L. P.; Procopiou, P. A. *Chem. Eur. J.* **2008**, *14*, 5716–5626. (j) van Otterlo, W. A. L.; de Koning, C. B. *Chem. Rev.* **2009**, *109*, 3743–3782. (k) Deraedt, C.; d'Halluin, M.; Astruc, D. *Eur. J. Inorg. Chem.* **2013**, 4881–4908.
- (4) (a) Giudici, R. E.; Hoveyda, A. H. *J. Am. Chem. Soc.* **2007**, *129*, 3824–3825. (b) Keitz, B. K.; Grubbs, R. H. *Organometallics* **2010**, *29*, 403–408. (c) Stenne, B.; Timperio, J.; Savoie, J.; Dudding, T.; Collins, S. K. *Org. Lett.* **2010**, *12*, 2032–2035. (d) Funk, T. W.; Berlin, J. M.; Grubbs, R. H. *J. Am. Chem. Soc.* **2006**, *128*, 1840–1846. (e) Schmidt, B.; Staude, L. *J. Org. Chem.* **2009**, *74*, 9237–9240. (f) Tiede, S.; Berger, A.; Schlesiger, D.; Rost, D.; Lühl, A.; Blechert, S. *Angew. Chem.* **2010**, *49*, 3972–3975.
- (5) (a) Stewart, I. C.; Ung, T.; Pletnev, A. A.; Berlin, J. M.; Grubbs, R. H.; Schrodi, Y. *Org. Lett.* **2007**, *9*, 1589–1592. (b) Berlin, J. M.; Campbell, K.; Ritter, T.; Funk, T. W.; Chlenov, A.; Grubbs, R. H. *Org. Lett.* **2007**, *9*, 1339–1342.
- (6) (a) Connon, S. J.; Blechert, S. *Bioorg. Med. Chem. Lett.* **2002**, *12*, 1873–1876. (b) Gulajski, L.; Michrowska, A.; Bujok, R.; Grela, K. *J. Mol. Catal. A* **2006**, *254*, 118–123. (c) Jordan, J. P.; Grubbs, R. H. *Angew. Chem., Int. Ed.* **2007**, *46*, 5152–5155. (d) Michrowska, A.; Gulajski, L.; Kaczmarek, Z.; Mennecke, K.; Kirschning, A.; Grela, K. *Green Chem.* **2006**, *8*, 685–688. (e) Burtscher, D.; Grela, K. *Angew. Chem., Int. Ed.* **2009**, *48*, 442–454. (f) Jordan, J. P.; Grubbs, R. H. *Angew. Chem., Int. Ed.* **2007**, *46*, 5152–5155. (g) Hong, S. H.; Grubbs, R. H. *J. Am. Chem. Soc.* **2006**, *128*, 3508–3509.
- (7) Representative examples: (a) Seiders, T. J.; Ward, D. W.; Grubbs, R. H. *Org. Lett.* **2001**, *3*, 3225–3228. (b) Ritter, T.; Day, M. W.; Grubbs, R. H. *J. Am. Chem. Soc.* **2006**, *128*, 11768–11769. (c) Chung, C. K.; Grubbs, R. H. *Org. Lett.* **2008**, *10*, 2693–2696. (d) Kuhn, K. M.; Bourg, J.-B.; Chung, C. K.; Virgil, S. C.; Grubbs, R. H. *J. Am. Chem. Soc.* **2009**, *131*, 5313–5320. (e) Savoie, T.; Stenne, B.; Collins, S. K. *Adv. Synth. Catal.* **2009**, *351*, 1826–1832. (f) Gatti, M.; Vieille-Petit, L.; Luan, X.; Mariz, R.; Drinkel, E.; Linden, A.; Dorta, R. *J. Am. Chem. Soc.* **2009**, *131*, 9498–9499. (g) Vieille-Petit, L.; Luan, X.; Gatti, M.; Blumentritt, S.; Linden, A.; Clavier, H.; Nolan, S. P.; Dorta, R. *Chem. Commun.* **2009**, 3783–3785. (h) Grisi, F.; Costabile, C.; Gallo, E.; Mariconda, A.; Tedesco, C.; Longo, P. *Organometallics* **2008**, *27*, 4649–4656.
- (8) (a) Grisi, F.; Mariconda, A.; Costabile, C.; Bertolasi, V.; Longo, P. *Organometallics* **2009**, *28*, 4988–4995. (b) Costabile, C.; Mariconda, A.; Cavallo, L.; Longo, P.; Bertolasi, V.; Ragone, F.; Grisi, F. *Chem. Eur. J.* **2011**, *17*, 8618–8629.
- (9) Stewart, I. C.; Benitez, D.; O'Leary, D. J.; Tkatchouk, E.; Day, M. W.; Goddard, W. A., III; Grubbs, R. H. *J. Am. Chem. Soc.* **2009**, *131*, 1931–1938.
- (10) Perfetto, A.; Costabile, C.; Longo, P.; Bertolasi, V.; Grisi, F. *Chem. Eur. J.* **2013**, *19*, 10492–10496.
- (11) Garber, S. B.; Kingsbury, J. S.; Gray, B. L.; Hoveyda, A. H. *J. Am. Chem. Soc.* **2000**, *122*, 8168–8179.
- (12) Complex *syn-10* was found to be stable for more than 1 month in C₆D₆, while *anti-10* decomposed after 2 weeks in C₆D₆.
- (13) (a) Sanford, M. S. Ph.D. Thesis, California Institute of Technology, Pasadena, CA, 2001. (b) Vougioukalakis, G. C.; Grubbs, R. H. *Organometallics* **2007**, *26*, 2469–2472. (c) Leuthäuser, S.; Schmidts, V.; Thiele, C. M.; Plenio, H. *Chem. Eur. J.* **2008**, *14*, 5465–5481.
- (14) Kolmer, A.; Kaltschnee, L.; Schimdt, V.; Peeck, L. H.; Plenio, H.; Thiele, C. M. *Magn. Reson. Chem.* **2013**, *51*, 695–700.
- (15) Credendino, R.; Falivene, L.; Cavallo, L. *J. Am. Chem. Soc.* **2012**, *134*, 8127–8135.
- (16) Ledoux, N.; Allaert, B.; Pattyn, S.; Mierde, H. V.; Vercaemst, C.; Verpoort, F. *Chem. Eur. J.* **2006**, *12*, 4654–4661.
- (17) Dichloro[1,3-bis(2-methylphenyl)-2-imidazolidinylidene](benzylidene)(tricyclohexylphosphine)ruthenium(II).
- (18) Dichloro[1,3-bis(2-methylphenyl)-2-imidazolidinylidene](2-isopropoxyphenylmethylene)ruthenium(II).
- (19) As an example, the kinetic plots of the sterically less demanding RCM reactions of **15** and **16**, promoted by *syn-10*, are reported in the Supporting Information.
- (20) [(4*R*,5*R*)-1,3-bis(2-methylphenyl)-4,5-diphenylimidazolin-2-ylidene]dichloro(benzylidene)(tricyclohexylphosphine)ruthenium(II).
- (21) Seiders, T. J.; Ward, D. W.; Grubbs, R. H. *Org. Lett.* **2001**, *3*, 3225–3228.
- (22) Hoye, T. R.; Zhao, H. *Org. Lett.* **1999**, *1*, 1123–1125.
- (23) (a) Li, Y.; Wu, Y.; Liang, L.; Li, Y.; Wu, G. *Chin. J. Polym. Sci.* **2010**, *28*, 55–62. (b) Vasilenko, I. V.; Frolov, A. N.; Kostjuk, S. V. *Macromolecules* **2010**, *43*, 5503–5507. (c) Liu, Q.; Wu, Yi-X.; Zhang, Y.; Yan, P.-F.; Xu, R.-W. *Polymer* **2010**, *51*, 5960–5969.
- (24) (a) Haskell, D. M.; Floyd, F. US Patent No. 4301315, 1981. (d) Evans, T. I.; Karas, L. J.; Rameswaran, R. US Patent No. 5877372, 1999.
- (25) (a) Alcántara, R.; Alcántara, E.; Canoira, L.; Franco, M. J.; Herrera, M.; Navarro, A. *React. Funct. Polym.* **2000**, *45*, 19–27. (b) Yoon, J. W.; Jhung, S. H.; Kim, T.-J.; Lee, H.-D.; Jang, N. H.; Chang, J.-S. *Bull. Korean Chem. Soc.* **2007**, *28*, 2075–2078.
- (26) (a) Burdette, G. W.; Schneider, A. I. US Patent No. 4398978, 1983. (b) Chickos, J. S.; Wentz, A. E.; Hillsheim-Cox, D. *Ind. Eng. Chem. Res.* **2003**, *42*, 2874–2877.
- (27) (a) Braddock, D. C.; Matsuno, A. *Tetrahedron Lett.* **2002**, *43*, 3305–3308. (b) Conrad, J. C.; Parnas, H. H.; Snelgrove, J. L.; Fogg, D. E. *J. Am. Chem. Soc.* **2005**, *127*, 11882–11883. (c) Vieille-Petit, L.; Clavier, H.; Linden, A.; Blumentritt, S.; Nolan, S. P.; Dorta, R. *Organometallics* **2010**, *29*, 775–788.
- (28) Meylemans, H. A.; Quintana, R. L.; Goldsmith, B. R.; Harvey, B. G. *ChemSusChem* **2011**, *4*, 465–469.
- (29) Clive, D. L. J.; Pham, M. P. *J. Org. Chem.* **2009**, *74*, 1685–1690.
- (30) (a) Hong, S. H.; Chlenov, A.; Day, M. W.; Grubbs, R. H. *Angew. Chem.* **2007**, *119*, 5240; *Angew. Chem., Int. Ed.* **2007**, *46*, 5148–5151. (b) Vehlow, K.; Gessler, S.; Blechert, S. *Angew. Chem.* **2007**, *119*, 8228–8231; *Angew. Chem., Int. Ed.* **2007**, *46*, 8082–8085.
- (31) For comparison, see ref 27c.
- (32) (a) Majumdar, K. C.; Rahaman, H.; Roy, B. *Curr. Org. Chem.* **2007**, *11*, 1339–1365. (b) Diederich, F.; Stang, P. J.; Tykwinski, R. R. *Modern Supramolecular Chemistry: Strategies for Macrocyclic Synthesis*; Wiley-VCH: Weinheim, Germany, 2008. (c) Cossy, J.; Arseniyadis, S.;

Meyer, C. *Metathesis in Natural Product Synthesis*; Wiley-VCH: Weinheim, Germany, 2010.

(33) Grisi, F.; Costabile, C.; Grimaldi, A.; Viscardi, C.; Saturnino, C.; Longo, P. *Eur. J. Org. Chem.* **2012**, 5928–5934.

(34) (a) Fürstner, A.; Thiel, O. R.; Ackermann, L. *Org. Lett.* **2001**, 3, 449–451. (b) Fürstner, A.; Ackermann, L.; Gabor, B.; Goddard, R.; Lehmann, C. W.; Mynott, R.; Stelzer, F.; Thiel, O. R. *Chem. Eur. J.* **2001**, 7, 3236–3253.

(35) This reaction proceeds through dimerization of substrate **33** at the monosubstituted double bond, as already described in ref 34.